The mucolipidosis IV Ca^{2+} channel TRPML1 (MCOLN1) is regulated by the TOR kinase

Rob U. Onyenwoke*[1], Jonathan Z. Sexton*, Feng Yan†, María Cristina Huertas Díaz‡, Lawrence J. Forsberg‡, Michael B. Major† and Jay E. Brenman†‡

*Biomanufacturing Research Institute and Technology Enterprise (BRITE), North Carolina Central University, Durham, NC 27707, U.S.A.
†Department of Cell Biology and Physiology, University of North Carolina-Chapel Hill, Chapel Hill, NC 27599, U.S.A.
‡Neuroscience Center, University of North Carolina-Chapel Hill, Chapel Hill, NC 27599, U.S.A.

Autophagy is a complex pathway regulated by numerous signalling events that recycles macromolecules and may be perturbed in lysosomal storage disorders (LSDs). During autophagy, aberrant regulation of the lysosomal Ca^{2+} efflux channel TRPML1 [transient receptor potential mucolipin 1 (MCOLN1)], also known as MCOLN1, is solely responsible for the human LSD mucolipidosis type IV (MLIV); however, the exact mechanisms involved in the development of the pathology of this LSD are unknown. In the present study, we provide evidence that the target of rapamycin (TOR), a nutrient-sensitive protein kinase that negatively regulates autophagy, directly targets and inactivates the TRPML1 channel and thereby functional autophagy, through phosphorylation. Further, mutating these phosphorylation sites to unphosphorylatable residues proved to block TOR regulation of the TRPML1 channel. These findings suggest a mechanism for how TOR activity may regulate the TRPML1 channel.

Key words: adenosine 5′-phosphate (AMP)-activated protein kinase, autophagy, lysosomal storage disease, mammalian target of rapamycin, mucolipidosis type IV, transient receptor potential channels.

INTRODUCTION

Autophagy is a pathway required for the degradation of cellular macromolecules [1,2]. During autophagy, double membrane-bound vesicles (autophagosomes) isolate the cytosolic material destined for degradation. Subsequently, autophagosomes fuse with late endosomes to form amphisomes [3,4]. Amphisomes then coalesce with lysosomes, leading to the formation of autolysosomes. Because lysosomes carry degradatory enzymes, the contents of amphisomes are broken down following autolysosome formation, with the produced metabolites partly feeding into catabolic pathways to satisfy the cell's energy demands [3,4]. Down-regulation of autophagy leads to the accumulation of misfolded proteins and is speculated to be involved in chronic or late-evolving diseases, such as neurodegenerative diseases, including Huntington's and Parkinson's disease [5,6].

In yeast, the cellular energy sensor SNF1 (sucrose non-fermenting 1), also known as AMPK (AMP-activated protein kinase), has a role in fully inducing autophagy [7]. However, mammalian studies demonstrate conflicting roles for AMPK in autophagy; there have been several studies indicating that AMPK is an inducer of autophagy [8–10], whereas there is also evidence that AMPK is an inhibitor of autophagy [11,12]. However, energetic stress undoubtedly stimulates both AMPK and autophagy, leading to the degradation of macromolecules and producing, for example, amino acids. Such substrates can then ultimately be funnelled into catabolic processes for energy generation whereas, at the same time, activating feedback loops that limit the extent of autophagy; for example, amino acids stimulate the target of rapamycin (TOR), which in turn, negatively regulates autophagy. TOR is directly activated by an upstream signalling pathway involving the TSC1–TSC2 (tuberous sclerosis complex) heterodimer. AMPK directly phosphorylates TSC2, thereby activating the TSC [13]. There is also evidence suggesting that AMPK might directly target and inhibit TOR [14] and AMPK-silencing (by $AMPK\alpha^{RNAI}$) does result in increased TOR activity [15].

While investigating the role of AMPK (by silencing its catalytic subunit, AMPKα, using RNAi) in autophagy and, more specifically, genes that are involved in autophagic dysfunction disorders [16–20]), we discovered evidence for a genetic interaction between AMPK and the lysosomal Ca^{2+} efflux channel TRPML1 [transient receptor potential mucolipin 1 (MCOLN1; UniProtKB–Q9GZU1)], also known as MCOLN1. Interestingly, mutations in *MCOLN1* (the name of the TRPML1 gene) are solely responsible for the human lysosomal storage disorder (LSD) MLIV (mucolipidosis type IV) [21,22].

First described in 1974 [23], MLIV (MIM 252650) is an autosomal recessive LSD. However, unlike most LSDs, the abnormal accumulation of macromolecules (sphingolipids, phospholipids and mucopolysaccharides) is not caused by a deficiency of lysosomal hydrolases nor related lysosomal proteins [23–30]. Rather MLIV is thought to result from abnormal sorting and/or transport of macromolecules along the late endocytic pathway [25,26]. This late endocytic defect is supported by experiments in which the uptake of radioactive phospholipids in cultured cells is increased in the lysosomes of MLIV compared with normal controls or even cells from individuals with other LSDs, including mucolipidosis types I–III [26,31]. More studies

Abbreviations: AMPK, AMP-activated protein kinase; FDR, false discovery rates; HEK, human embryonic kidney; IP, immunoprecipitation; KD, kinase-dead; LC3, light chain 3; LSD, lysosomal storage disorder; MCOLN1, mucolipin 1; MLIV, mucolipidosis type IV; ML-SA1, mucolipin synthetic agonist 1; PI, protease inhibitor; PKA, protein kinase A; RT, room temperature; S6K, S6 kinase; SNF1, sucrose non-fermenting 1; TOR, target of rapamycin; TRP, transient receptor potential; TSC, tuberous sclerosis complex; WT, wild-type.

[1] To whom correspondence should be addressed (email ronyenwo@nccu.edu).

using a mouse model for MLIV have also supported a late endocytic pathway defect [32–34].

Since TRPML1 pathophysiology results in a very specific LSD [25,26], we attempted to determine if the dysregulation of AMPK signalling might play a role in MLIV by leading to a loss of balance between component transport into lysosomes and their catabolism. However, a MS-based experiment indicated that TOR and not AMPK might be directly regulating TRPML1, even though we initially detected a genetic interaction between *AMPK* and *MCOLN1*. We further characterized the MS-identified TOR–TRPML1 interaction and provide evidence that TOR regulates TRPML1 through phosphorylation. The present study provides additional mechanistic information on the regulation of autophagy and may provide a framework to better understand MLIV and other lysosomal and autophagic-related diseases.

EXPERIMENTAL

Materials

All chemicals were of an analytical grade and, unless otherwise noted, from Sigma-Chemical or Fisher Scientific. [γ-32P]ATP (specific activity 3000 Ci/mmol) was from PerkinElmer. The MCOLN1 peptides (RRKCGRDPSEEHSLLVN, RRKCGRDPAEEHALLVN, RRKCGRDPAEEHSLLVN, RRKCGRDPSEEHALLVN) were synthesized by the UNC High-Throughput Peptide Synthesis and Array Facility. MHY1485 was synthesized and the compound identity was verified by LC–MS and NMR, in-house at North Carolina Central University, as previously described [35]. The antibodies used were as follows: anti-LC3 [1:1000 (in milk); MBL International], anti-c-Myc [1:40 dilution for 1 mg/ml lysate for immunoprecipitation (IP); Developmental Studies Hybridoma Bank, University of Iowa], anti-α-tubulin (clone B-5-1-2; Sigma–Aldrich) and anti-GFP (A11122 for IP and A6455 for Western; Molecular Probes). pEGFPC2-MCOLN1 [full-length, wild-type (WT), human and cloned into the *Eco*RI and *Sal*I sites] was a generous gift from R. Puertollano (National Institute of Health, Bethesda, Maryland) and is as previously described [36]. The myc-TOR, kinase-dead (KD) myc-TOR and RFP-LC3 plasmids were from Addgene.

Cell culture and transient transfection

Unless otherwise noted, human embryonic kidney (HEK)293T cells were cultured in complete DMEM (Dulbecco's modified Eagle's medium; Life Technologies) containing 10% FBS (Atlanta Biologicals) at 37 °C in 5% CO_2.

For the transient expression of the myc-TOR protein, the cells were plated 24 h before the experiments in 15-cm dishes and then transfected with the plasmid using Lipofectamine 2000 (1 μg of DNA per 2 μl; Invitrogen) following the manufacturer's protocols. Note: for some kinase assays, myc-TOR was replaced with KD myc-TOR. Cells were then harvested, lysed in buffer A (50 mM Tris/HCl, pH 7.5, protease [Sigma–Aldrich] and phosphatase [Sigma–Aldrich] inhibitor cocktails and benzonase nuclease) plus 1.0% Triton X-100 with shaking for 1 h (4 °C) and centrifuged at 16000 ***g*** for 10 min (4 °C). myc-tagged TOR was purified from the supernatants via IP using the anti-c-Myc antibody at a 1:40 dilution for 1 mg/ml lysate and A/G agarose (Thermo Fisher Scientific) according to the manufacturer's instructions and as previously described [37].

Affinity purification and MS

IP–MS of HEK293T cells transiently transfected with human EGFP–WT–MCOLN1 and treated with 200 nM rapamycin, 200 μM $CoCl_2$ or DMSO (vehicle) were performed in duplicate. Briefly, protein lysates from the transfected cell lines were lysed in 100 mM Tris/HCl (pH 8.0), 100 mM NaCl, 2% Triton X-100, 1 mM DTT, benzonase nuclease (Thermo Fisher Scientific) and protease (Sigma–Aldrich) and phosphatase (Sigma–Aldrich) inhibitor cocktails and subjected to IP with an anti-GFP antibody (1:500 dilution; Molecular Probes). Following an on-beads digestion with a FASP Protein Digestion kit (Expedeon) and sequencing grade-modified trypsin (Promega), phosphopeptide enrichment was performed from total peptide pools using a Ti-oxide column (Titansphere Phos-TiO kit, GL Sciences).

The identity of the eluted peptides was determined using an in-line LTQ-Orbitrap Velos mass spectrometer (Thermo Scientific). The ion source was operated at 2.0–2.4 kV with the ion transfer tube temperature set at 275 °C. Full MS scan (300–2000 *m/z*) was acquired in Orbitrap at 60000 resolution setting; data-dependent MS2 (tandem mass spectrometry) spectra were acquired in Linear Trap Quadropole (LTQ) by collision-induced dissociation with the 20 most intense ions. Precursor ions were selected on the basis of charge states (1, 2 or 3) and intensity thresholds (above 2000) from the full scan; dynamic exclusion (one repeat during 30 s, with a 60-s exclusion time window) was also taken into account.

All raw data spectra were searched using SorcererTM-SEQUEST® (Sage N Research) and the Transproteomic Pipeline. Data were searched against the human UniProtKB/Swiss-Prot sequence database (Release 2011_08) supplemented with common contaminants and further concatenated with its reversed copy as a decoy (40494 total sequences). Search parameters used were a precursor mass between 400 and 4500 amu, up to two missed cleavages, precursor-ion tolerance of 3 amu, accurate mass binning within PeptideProphet, semi-tryptic digestion, a static carbamidomethyl cysteine modification, variable methionine oxidation and variable phosphorylation of serine, threonine and tyrosine residues. False discovery rates (FDR) were determined by ProteinProphet and minimum protein probability cut-offs resulting in a 1% FDR were selected individually for each experiment.

Site-directed mutagenesis

Site-directed mutagenesis of *MCOLN1* was carried out using the QuikChange II XL Site-Directed Mutagenesis kit (Agilent Technologies). The primers utilized in the mutagenesis are listed in the Supplementary Materials and Methods.

Fura-2 Ca^{2+} imaging

Cells were loaded with 5 μM Fura-2 AM (Life Technologies) in the culture medium at 37 °C for 60 min. The cells were then washed three times with modified Tyrode's solution {150 mm NaCl, 5 mm KCl, 2 mm $CaCl_2$, 1 mm $MgCl_2$, 10 mM $NaHCO_3$, 10 mm glucose (pH 7.4) [38,39]} and imaged in wide-field fluorescence mode in a 96-well format with a 20×/0.75 NA Olympus UPlanApo objective lens using a BD Pathway 855 bioimager equipped with 37 °C environmental control, liquid handling and a Nikon A1 confocal microscope (Becton Dickenson) within 1 h of processing. EGFP was imaged with a 488/10 nm band-pass excitation filter and a 515 long-pass emission filter. Ratiometric Fura-2 AM (excitation 340 and 380 nm, emission 435 nm long-pass, ratio = 340/380) imaging was used to monitor changes in intracellular [Ca^{2+}] upon

Table 1 ***AMPKα*** **RNAi and** ***AMPKα*** **loss-of-function rescue by** ***MCOLN***

Transgene or loss-of-function mutation	*AMPKα* RNAi rescue (% expected)	*AMPKα* loss-of-function allele 1 rescue (number rescue/total number scored)	*AMPKα* loss-of-function allele 2 rescue (number rescue/total number scored)
UAS-S6k (DN)	Yes (11)	Yes (14/130)	Yes (23/122)
UAS-TOR (DN)	Yes (13)	No (0/68)	No (0/42)
UAS-MCOLN (WT)	No (0/1312)	No (0/1081)	No (0/231)
MCOLN[1]	Yes (16)	Yes (8/98)	Yes (6/80)
MCOLN[2]	Yes (14)	Yes (6/122)	Yes (10/78)
UAS-MCOLN-RNAi	Yes (18)	Yes (8/130)	Yes (10/156)
UAS-AMPKα	Yes (100)	Yes (22/65)	Yes (36/75)
UAS-AMPKγ	No	No (0/63)	No (0/94)
UAS-GFP	No	No (0/52)	No (0/77)

stimulation [38,40]. Laser-based autofocus was performed in each well prior to the collection of EGFP and Fura-2 images. ML-SA1 (10 μM, a direct and specific TRPML1 agonist) and ionomycin (1 μM) were used to induce Ca^{2+} flux and as a positive control to induce a maximal response respectively. Time-zero GFP and Fura-2 ratio images were collected prior to the addition of compounds/vehicle controls in 10–100 μl well-volumes using a single-channel automated pipettor followed by the acquisition of 50 additional Fura-2 ratiometric images at approximately three images per second. CellProfiler was used for image processing to tabulate calcium flux traces on a per-cell basis [41].

Kinase assays

Kinase assays were performed according to previously described methods [42,43]. Briefly, the assays with myc-tagged TOR were performed at room temperature (RT, 25 °C) in 25 μl of reaction mixture containing 3–12 μg of protein in kinase buffer (50 mM Hepes, pH 7.0, 75 mM NaCl, 5 mM sodium acetate, 5 mM magnesium chloride, 1 mM DTT, 8 % glycerol, 0.1 mM EDTA, 200 μM AMP and ATP and 2 μCi of [γ-^{32}P]ATP) with or without the peptide. After a 30-min incubation period, the reaction mixtures were counted in a scintillation counter.

In vitro phosphorylation

HEK293T cells were transfected with either WT full-length GFP–MCOLN1 or full-length GFP–MCOLN1$^{S572A/S576A}$ (S572,576/AA) and myc-TOR (WT), lysed in phosphorylation buffer [50 mM Tris/HCl (pH 7.4), 100 mM NaCl, 0.5 mM DTT and 10 mM $MgCl_2$] supplemented with 2 % (v/v) Triton X-100 and protease and serine/threonine phosphatase inhibitors, incubated with or without 200 nM rapamycin (20 min, RT), then labelled with 2 μCi of [γ-^{32}P]ATP (30 min, RT) and immunoprecipiated using the anti-GFP antibody and Protein A/G agarose (washed three times with the phosphorylation buffer). Samples were eluted using Laemmli buffer, separated by electrophoresis, stained with Coomassie Brilliant Blue and subjected to autoradiography.

Western blotting

Protein lysates for immunoblotting were prepared by suspending cell pellets in lysis buffer A plus 1.0 % Triton X-100 with shaking for 1 h (4 °C) and centrifuged at 16000 ***g*** for 10 min (4 °C) in 1.5-ml microfuge tubes. Supernatants were collected and protein concentrations were determined using the Bio-Rad DC protein assay. Proteins (50 μg) were then boiled in loading buffer and subjected to SDS/PAGE (Invitrogen), followed by Western analyses using the primary antibodies. Secondary antibodies (IRDye infrared antibodies; LI-COR Biosciences) were used at a dilution of 1:2000. Scanning, analysing and quantification of blots were performed via the Odyssey Infrared Imaging System (LI-COR Biosciences). Three or more independent experiments were performed for all immunoblotting data.

Fly stocks, crosses and rescue experiments

Drosophila melanogaster strains obtained from the Bloomington Stock Center included the following: w^{1118}, *Act-GAL4, Tub-GAL4*, *Ubi-GAL4*, $trpml^{1}$ (referred to as *MCOLN*[1] in the present study), *UAS-TRPML*^{RNAI}, *UAS-AMPKα*^{RNAI}, the $SNF1A^{1}$ and $SNF1A^{3}$ mutants, *UAS-SNF1A*, $AMPK^{K57A}$, *UAS-S6k.KQ*, *UAS-Tor.TED* and *UAS-GFP*. *UAS-SNF4* and the $trpml^{2}$ lines (referred to as *MCOLN*[2]) were gifts from D. Kretzschmar (Oregon Health and Science University) and C. Montell (University of California) respectively. All flies were maintained at ∼25 °C in yeast-cornmeal vials and all crosses were also performed in cornmeal-yeasted vials.

For the *AMPKα* RNAi rescue experiments, males carrying a transgene or loss-of-function mutation on the second or third chromosome were mated to virgin females carrying a *GAL4* (either *Tub-GAL4* or *Act-GAL4* respectively). From these crosses, male progeny carrying the transgene or loss-of-function mutation and the *GAL4* were mated to virgin females carrying *UAS-AMPKα*^{RNAI}. The progeny from this second cross were then scored for rescue, i.e. viable adult flies in spite of AMPKα RNAi knockdown.

For the *AMPKα* loss-of-function rescue experiments, males carrying a transgene or loss-of-function mutation on the second or third chromosome were mated in parallel to virgin females from both the $SNF1A^{1}$ and the $SNF1A^{3}$ loss-of-function lines. The male progeny from both of these crosses were scored for rescue, i.e. viable adult flies in spite of carrying the lethal loss-of-function mutation/phenotypically, non-bar-eyed males.

Statistical analyses

For all quantified experiments, data are presented as mean ± S.E.M. ANOVA was used to determine the statistical significance with significance set at 0.05. For Western blot quantification, independent experiments (cell preparation, cell harvest and SDS/PAGE/transfer) were performed three times (unless otherwise noted). Indirect immunofluorescent detection of secondary antibody (LI-COR) was scanned and standardized to an

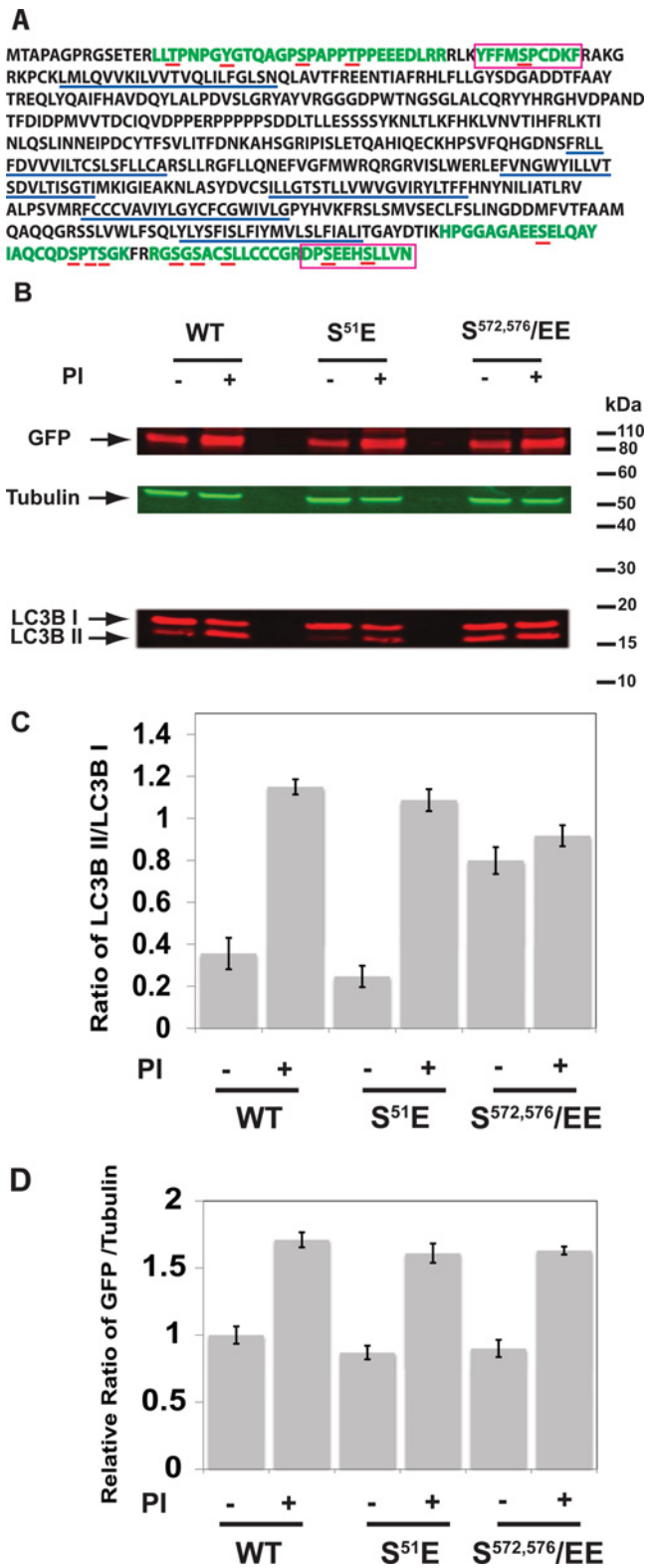

Figure 1 The phosphorylation state of C-terminal tail serine residues of TRPML1 (Ser^{572} and Ser^{576}) regulate autophagy

(**A**) MS identified unique phosphopeptides in the complete sequence of TRPML1 (UniProtKB – Q9GZU1) that are absent after rapamycin treatment. The identified phosphopeptide sequences are in green, phospho-residues are underlined in red and unique peptides absent when rapamycin was used during cell culture are boxed in magenta. The six predicted transmembrane domains of TRPML1 are included underlined in blue. (**B**) HEK293T cells transfected with either EGFP-tagged WT–MCOLN1; the S51E construct, MCOLN1^{S51E}; or the S572E/S576E construct, MCOLN1$^{S572E/S576E}$ were treated with or without lysosomal PIs [E-64d + Pepstatin A (10 μg/ml of each)] for 12 h. The cells were then lysed and immunoblotted with anti-LC3, anti-GFP [to quantify the GFP–MCOLN1 constructs (~93 kDa)] and anti-α-tubulin (n=4). (**C**) The quantification of the ratio of LC3BII to LC3BI from (**B**). A ratio of '1' would indicate equal quantities of LC3BII and LC3BI. (**D**) The quantification of the relative ratio of GFP to α-tubulin.

internal standard (tubulin) to calculate and quantify arbitrary units using the Odyssey Infrared Imaging System with a representative Western blot shown in each Figure.

RESULTS

MCOLN1 genetically interacts with *AMPK*

We initially screened through known *Drosophila* mutations that produce neurodegenerative phenotypes (including *MCOLN*) [18,44] that might interact with *AMPK* mutants, which also produce neural degeneration-like phenotypes [16–20]. Although there are multiple genes that encode TRPML channels in mammals (*MCOLN1*, *MCOLN2* and *MCOLN3*, also known as *TRPML1*, *TRPML2* and *TRPML3*), there is only a single *MCOLN* (*TRPML*) gene in *Drosophila* with two previously characterized gene deletion lines available for study [45]. We therefore utilized *Drosophila* genetics to examine the functional consequences of altered TRPML activity *in vivo* in a less genetically redundant system than the TRPML vertebrate genome.

We investigated the relationship between *MCOLN* and *AMPK* gene functions by reducing AMPKα activity through the use of a transgenic RNAi-based expression system. This previously characterized AMPK RNAi system phenocopies genetic loss of AMPKα and only allows *Drosophila* development to reach the late pupal/pharate adult stage without producing eclosing adults [46,47]. Through the use of this transgenic RNAi-based expression system [46,47], we determined that introducing a single *MCOLN* loss-of-function mutation for either MCOLN allele rescued otherwise lethal AMPKα knockdown animals to viability/eclosion (Table 1). In addition, heterozygous *MCOLN* loss-of-function alleles were able to rescue previously published [20] null *AMPKα* lethal loss-of-function alleles to viability as well, an effect otherwise only observed with dominant-negative S6 kinase (S6K; in the TOR pathway), which is known to antagonize AMPK function [48]. In support of these results, increased TRPML1 expression did not rescue AMPKα knockdown or loss-of-function animals but actually significantly antagonized (decreased) the viability of the KD –AMPKα animal [46] (Supplementary Table S1).

Phosphopeptide purification and MS of TRPML1 identifies novel phospho-serine sites

Based upon the finding that *MCOLN1* and *AMPK* genetically interact, we sought to identify possible sites of interaction (phosphorylation sites) in the TRPML1 protein. Originally, we hypothesized that AMPK might directly phosphorylate TRPML1 to regulate its autophagic function. Using HEK293T cells, we transiently transfected human EGFP–WT–MCOLN1, which leads to its protein localization in late endosomes and lysosomes (its physiological localization), in addition to the plasma membrane (Supplementary Figure S1) [49–51]. We subsequently treated the transfected cells with rapamycin (a TOR antagonist), $CoCl_2$ (an AMPK activator [47,52]) or DMSO (vehicle) followed by IP with a GFP antibody to look for phosphorylation changes in

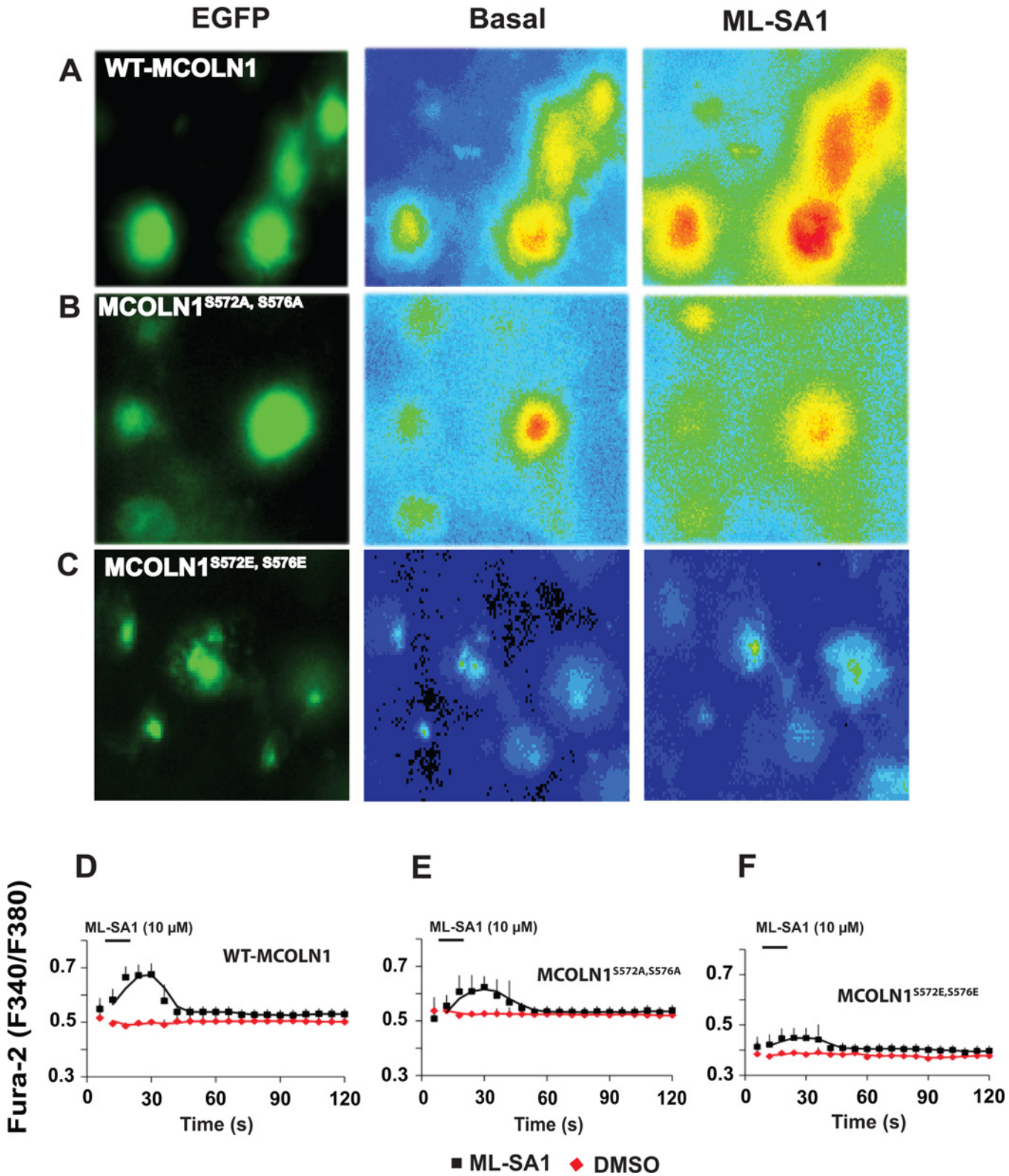

Figure 2 The S572E/S576E TRPML1 phosphomimetic is non-responsive to TRPML1 agonists

Intracellular Ca^{2+} ($[Ca^{2+}]_i$) was investigated using HEK293T cells transfected with either (**A**) EGFP-tagged WT–MCOLN1; (**B**) the S572A/S576A construct, $MCOLN1^{S572A/S576A}$; or (**C**) the S572E/S576E construct, $MCOLN1^{S572E/S576E}$ and the TRPML1 agonist ML-SA1. TRPML1 protein expression was monitored by the presence of an EGFP signal measured at an excitation of 488 nm (F_{488}). $[Ca^{2+}]_i$ was monitored with Fura-2 ratios (F_{340}/F_{380}). The extracellular Ca^{2+} ($[Ca^{2+}]_o$) was 2 mM and the [ML-SA1] was 10 μM. (**D**–**F**) In WT–MCOLN1- and $MCOLN1^{S572A/S576A}$ -transfected cells (**D** and **E**), the Fura-2 ratios increased in response to ML-SA1 and gradually recovered. The change in the Fura-2 ratio for $MCOLN1^{S572E/S576E}$ (**F**) was negligible.

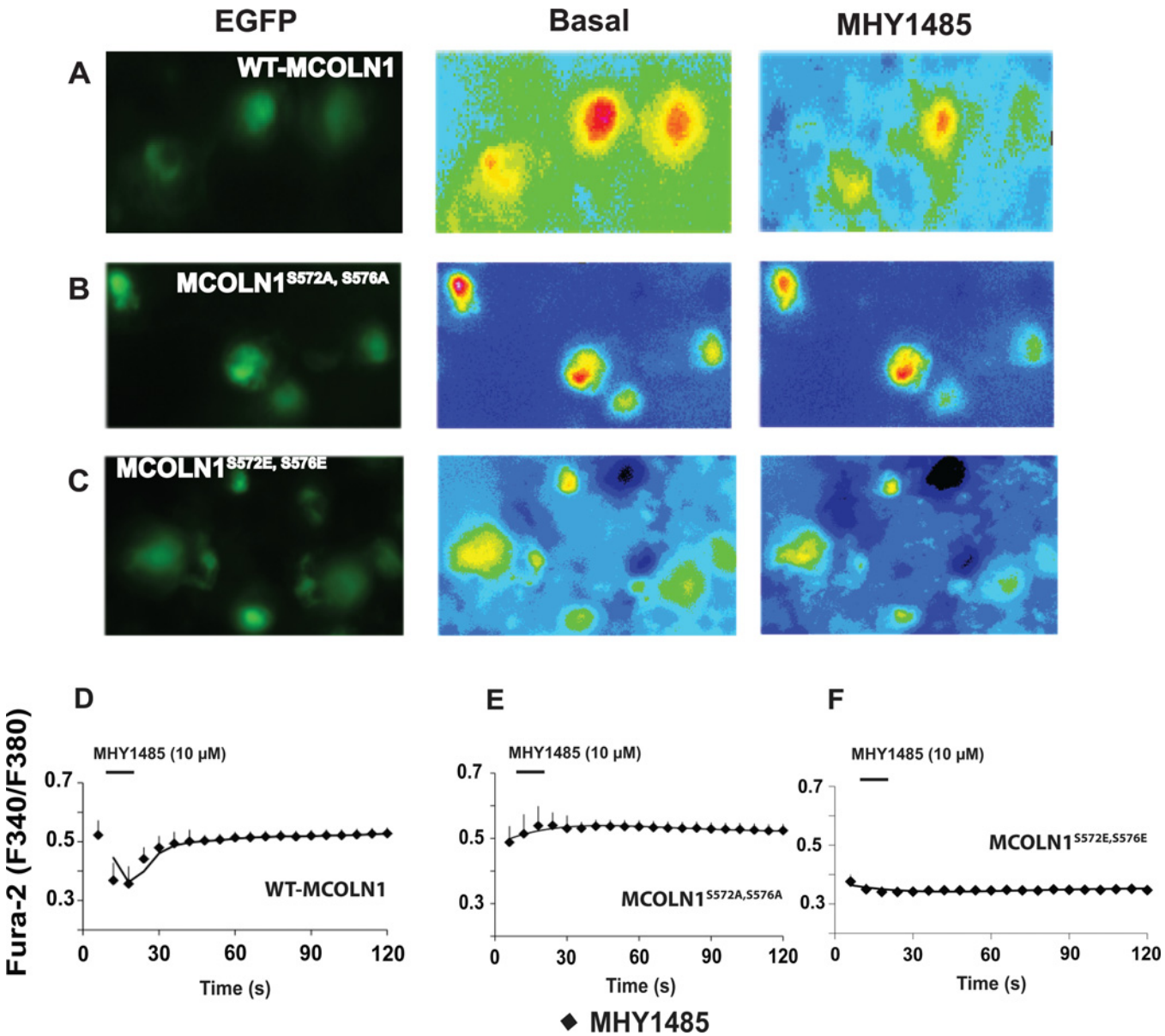

Figure 3 The TOR agonist MHY1485 can deactivate the TRPML1 channel through the phosphorylation of Ser^{572} and Ser^{576}

Intracellular Ca^{2+} ($[Ca^{2+}]_i$) was investigated in HEK293T cells transfected with either (**A**) EGFP-tagged WT–MCOLN1; (**B**) the S572A/S576A construct, MCOLN1$^{S572A/S576A}$; or (**C**) the S572E/S576E construct, MCOLN1$^{S572E/S576E}$. TRPML1 protein expression was monitored by the presence of an EGFP signal measured at an excitation of 488 nm (F_{488}). $[Ca^{2+}]_i$ was monitored with Fura-2 ratios (F_{340}/F_{380}). The extracellular Ca^{2+} ($[Ca^{2+}]_o$) was 2 mM and the [MHY1485] was 10 μM. (**D**–**F**) In the WT–MCOLN1-transfected cells (**D**), the Fura-2 ratios decreased in response to MHY1485 and gradually recovered whereas the Fura-2 ratios of the MCOLN1$^{S572A/S576A}$ -transfected cells (**E**) were not affected. The change in the Fura-2 ratios for MCOLN1$^{S572E/S576E}$ (**F**) was negligible; however, these ratios were well below the MCOLN1$^{S572A/S576A}$ -transfected cells and the recovered WT–MCOLN1-transfected cells.

TRPML1 in response to these stimuli. After peptide digestion, followed by phosphopeptide enrichment, the peptides were subjected to MS, whereupon several phosophopeptides were identified (Figure 1A; Supplementary Table S2). Interestingly, two peptides (one N-terminal peptide, containing one predicted phospho-serine residue and one C-terminal peptide, containing two predicted phospho-serine residues) were absent from the peptide pool from the cells treated with the TOR inhibitor rapamycin but present with the other treatments. Based on these results, we proceeded to further investigate the functional consequences of mutating these three serine residues to alanine (non-phosphorylatable) or glutamic acid (a phosphomimetic) residues individually or, in the case of the C-terminal peptide containing two serine residues, both residues. In addition, these findings suggested that TOR, and not AMPK, might be a more direct regulator or TRPML1.

Phosphorylation of the C-terminal TRPML1 serine residues results in decreased autophagic flux

To ascertain the extent of functional autophagy as a metric of TRPML1 activity, we assessed the relative level of microtubule-associated protein 1A/1B-light chain 3 (LC3). LC3 is one of

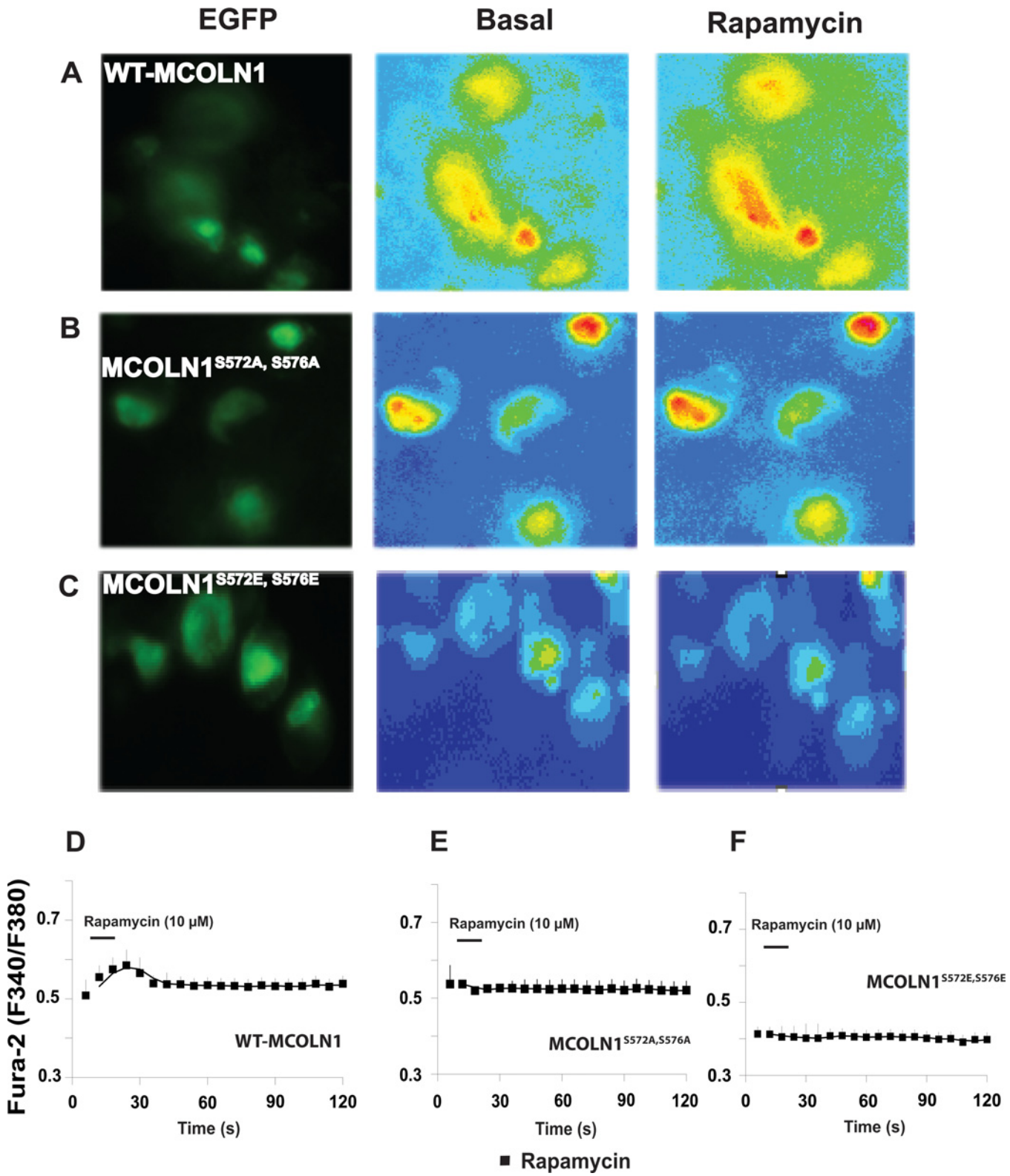

Figure 4 S572A/S576A TRPML1 and the S572E/S576E TRPML1 phosphomimetic are non-responsive to rapamycin

Intracellular Ca^{2+} ($[Ca^{2+}]_i$) was investigated using HEK293T cells transfected with either (**A**) EGFP-tagged WT–MCOLN1; (**B**) the S572A/S576A construct, $MCOLN1^{S572A/S576A}$; or (**C**) the S572E/S576E construct, $MCOLN1^{S572E/S576E}$ and the TOR antagonist rapamycin. TRPML1 protein expression was monitored by the presence of an EGFP signal measured at an excitation of 488 nm (F_{488}). $[Ca^{2+}]_i$ was monitored with Fura-2 ratios (F_{340}/F_{380}). The extracellular Ca^{2+} ($[Ca^{2+}]_o$) was 2 mM and the [rapamycin] was 10 μM. (**D**–**F**) In the WT–MCOLN1-transfected cells (**D**), the Fura-2 ratio increased in response to rapamycin and gradually recovered. The changes in the Fura-2 ratios for $MCOLN1^{S572A/S576A}$ and $MCOLN1^{S572E/S576E}$ (**E** and **F**) were negligible.

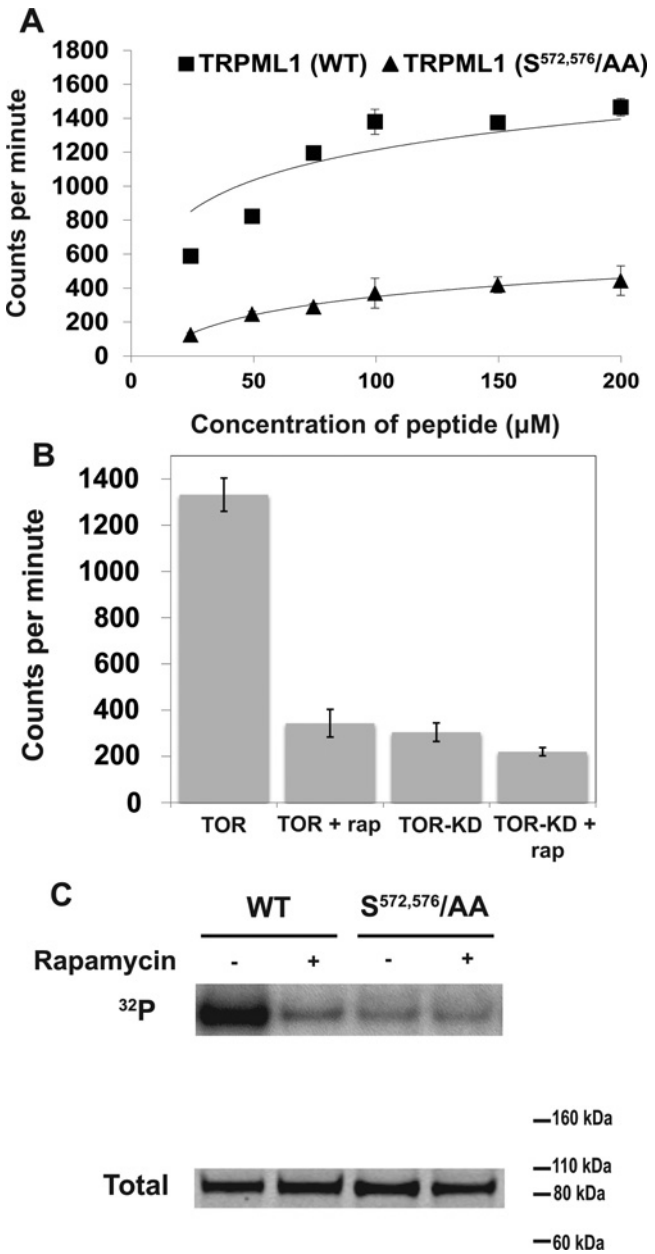

Figure 5 TRPML1 is phosphorylated by mTOR on Ser^{572} and Ser^{576}

(**A**) Kinase assays were performed with purified WT myc-tagged TOR. Synthesized TRPML1 peptides (WT–TRPML1 and TRPML1$^{S572A/S576A}$; no phosphorylatable residues) were compared as TOR substrates. The kinase assays were performed with varying amounts of the substrate peptides to measure the kinetics (n=3). (**B**) Kinase assays were performed with either purified WT–TOR or KD–TOR and the WT–TRPML1 peptide (n=3). The HEK293T cells expressing the TOR constructs were cultured either in the presence or in the absence of 200 nM rapamycin for 12 h before purification. (**C**) *In vitro* phosphorylation of WT full-length EGFP–TRPML1 (WT) or full-length EGFP–TRPML$^{S572A/S576A}$ (S572,576/AA). HEK293T cells transfected with either construct [all cells were additionally transfected with myc-TOR (WT)] were lysed, incubated with or without 200 nM rapamycin (20 min), labelled with [γ-^{32}P]ATP (30 min) and immunoprecipiated with an anti-GFP antibody. Samples were separated by electrophoresis, stained with Coomassie Brilliant Blue (total, lower panel) and subjected to autoradiography (^{32}P, upper panel). Staining with Coomassie Brilliant Blue showed similar levels of fusion protein in each lane.

the most selective markers for autophagosomes [53]. Upon induction of autophagy, LC3-I becomes lipid conjugated with phosphatidylethanolamine (PE) into LC3-II, which is then targeted to the membrane of autophagosomes [54,55]. Although the relative abundance of LC3-II does correlate with the formation of autophagosomes, it does not indicate whether these autophagosomes are capable of completing functional autophagy. Lysosomal protease inhibitors (PIs), for example, pepstatin A and E-64d, are therefore utilized to allow for the formation of autolysosomes but to partially prevent the functional completion of autophagy [56,57]. In this manner, increased complete autophagy would lead to increased levels of LC3-II in the presence of the PIs compared with the absence of PIs, whereas decreased autophagic flux/turnover would result in a similar level of LC3-II with or without the PIs [56].

Using this assay, the combined S572E/S576E phosphomimetic mutation of TRPML1 resulted in an inhibition of autophagic degradation, as evidenced by the increased accumulation of LC3-II (the membrane-bound form of LC3 that is characteristic of autophagosomes) that was similar with and without the PIs; whereas the S51E variant (and S572A/S576A and S51A variants) of TRPML1 resulted in no significant increase in LC3-II accumulation (Figures 1B–1D, Supplementary Figure S2) compared with the WT with or without the PIs. These results suggested that the C-terminal phospho-serines, and not the N-terminal phospho-serine, had profound effects on TRPML1 function.

Calcium imaging indicates that phosphorylation of the C-terminal TRPML1 serine residues results in decreased channel activity

To further ascertain if phosphorylation (at Ser^{572} and Ser^{576}) may regulate autophagy through the Ca^{2+} efflux activity of the TRPML1 channel, we performed real-time calcium imaging using the Ca^{2+}-specific reagent Fura-2 AM [38] in HEK293T cells transfected with either EGFP–WT–MCOLN1, the S572E/S576E construct or the S572A/S576A construct. This technique relies upon the fact that the recombinant overexpressed TRPML1 channel is partially localized to the plasma membrane, allowing for an easy demonstration of the Ca^{2+} influx activity of the channel from the media when activated using an appropriate agonist [38,51]. The results illustrate that the S572E/S576E variant was virtually non-responsive to the TRPML1 agonist ML-SA1 (mucolipin synthetic agonist 1, a known specific agonist for TRPML1 [39]) in comparison with both the WT and the S^{572}A/S^{576}A variants (Figure 2, Supplementary Figures S3A, S3B and S4A), whereas the single variants (S572A, S572E, etc.) behave similarly to WT (Supplementary Figure S5A and S5B). Because of the differential response profile with the S^{572}E/S^{576}E variant [and not S572E or S576E (or S51E) alone], the S572A/S576A and S572E/S576E variants became our primary focus.

When MHY1485 (a TOR agonist previously demonstrated to inhibit autophagy [35]) was utilized in the same assay described above, the activity of the S572A/S576A construct was unaffected by the compound even though the WT channel was obviously inhibited (Figures 3A and 3B; Supplementary Figure S4B). Because rapamycin treatment led to our initial discovery of these novel phospho-serine residues, we also assayed the effect of rapamycin on these channels. Although rapamycin did activate the WT channel, the response compared with the basal activation was not statistically significant and again the S572A/S576A construct was not obviously affected (Figures 4A and 4B; Supplementary Figure S4C). These results again indicated that TOR may regulate the TRPML1 channel through the phosphorylation of these two C-terminal serine residues.

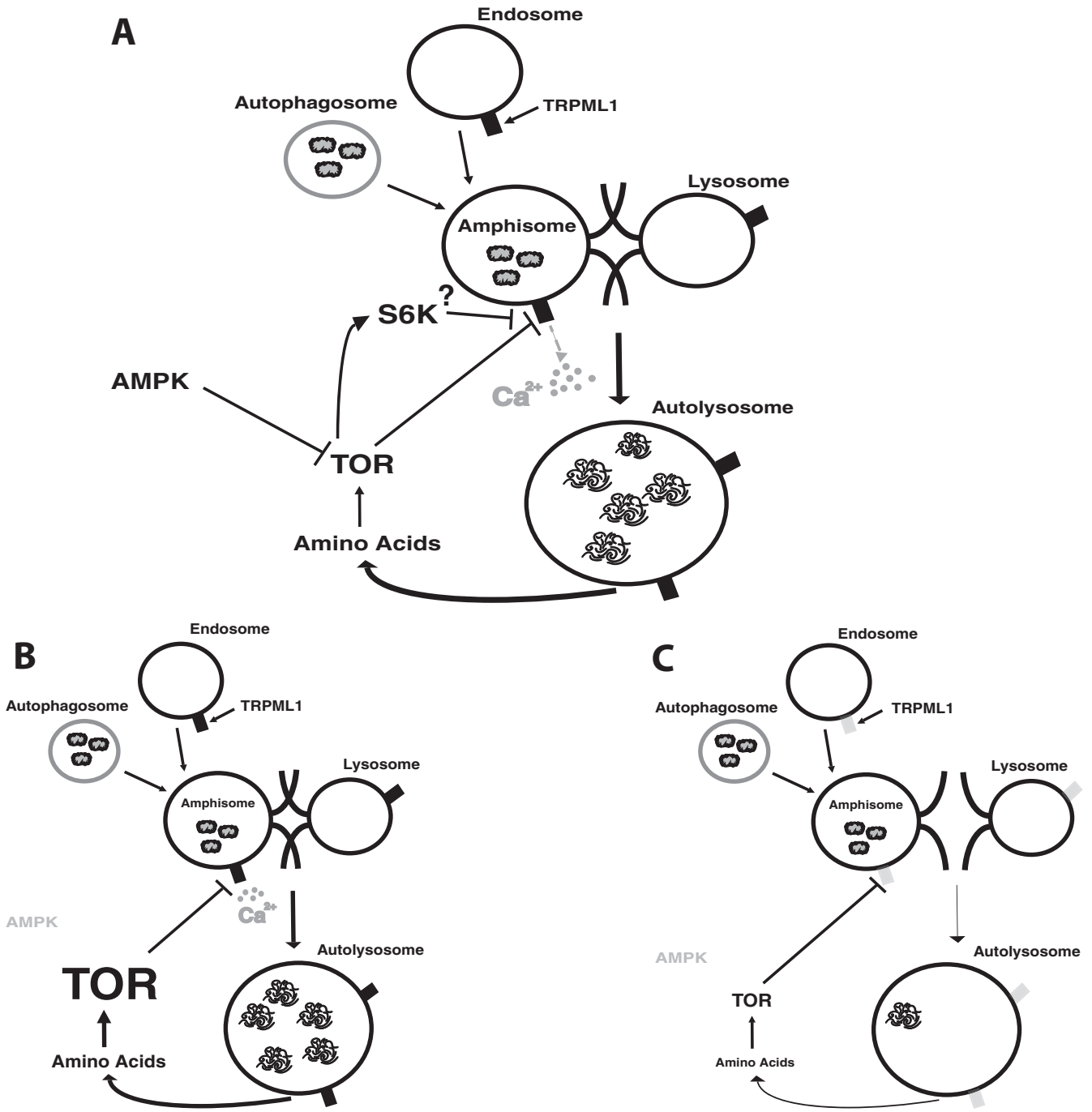

Figure 6 mTOR inhibits TRPML1 activity during autophagy through phosphorylation

The model in (**A**) explains how mTOR, AMPK and TRPML1 possibly interact whereas the models presented in (**B**) and (**C**) attempt to explain: (1) why loss of AMPK activity alone is lethal in relation to (2) why loss of both AMPK and TRPML1 activity resulted in the limited viability in the presented *Drosophila* genetic studies that served as the basis for the present work respectively. (**A**) When active (for example, under starvation conditions), AMPK inhibits mTOR (or its downstream effector molecule S6K1) activity, which in turn modulates TRPML1 activity in a feedback loop (i.e., inactive/less active mTOR leads to increased TRPML1 activity; however, activating TRPML1 increases autophagy, leading to increased amino acid production and activating mTOR; a feedback loop that regulates/modulates mTOR, AMPK and TRPML1 activity). (**B**) In the absence of only AMPK activity [due to a condition/state where there is a loss of AMPK activity and not simply due to nutrient-rich conditions, which can be simply explained by the feedback loop in (**A**)], negative TOR regulation is significantly lessened (increased TOR activity), probably contributing to the loss of viability that occurs when AMPK activity is lost, i.e. a complete loss of AMPK activity is known to be developmentally lethal [46,47]. Please note: due to increased mTOR activity, there would also probably be a significant accumulation of amphisomes and lysosomes, possibly leading to the neurodegeneration phenotype often accompanying a loss of functional AMPK [16–20] (not pictured). (**C**) In the absence of both functional AMPK and TRPML1, TOR activity is balanced because (1) the negative regulation of AMPK activity is absent (**A**), but (2) the positive regulation involving autophagy, i.e. the production of nutrients, such as amino acids, is also absent, leading to a limited viability in the absence of AMPK activity [58,59] (refer to Table 1 for the viability results) and explaining the *Drosophila* genetic study results described in the present work.

In vitro phosphorylation and kinase assays support a role for the direct phosphorylation of the TRPML1 channel by the TOR kinase

To determine whether TOR could directly phosphorylate TRPML1 *in vitro*, kinase assays were performed to monitor the incorporation of ^{32}P into modified versions of the TRPML1 C-terminal peptide (refer to the 'Experimental' for the exact sequences of these peptides; Figures 1A, 5A and 5B; Supplementary Figure S6) [42,43]. In brief, either Ser^{572} or Ser^{576} (or both) was replaced with an unphosphorylatable alanine residue in the C-terminal TRPML1 peptide for the ^{32}P incorporation assays. The kinase assays revealed that the C-terminal peptide is indeed a robust TOR substrate (Figures 5A and 5B), whereas versions of the peptide altered at one or both of the putative serine residues (S572A/S576A) were relatively poor TOR substrates (Supplementary Figure S6).

To further illustrate the direct phosphorylation of TRPML1 by TOR, cells transfected with either the full-length WT channel or the full-length S572,576/AA mutant were ^{32}P-labelled in either the presence or the absence of rapamycin (Figure 5C). The channel was then immunoprecipitated using anti-GFP antibody and visualized by SDS/PAGE and autoradiography. The WT channel was significantly more labelled compared with the S572,576/AA mutant and rapamycin treatment decreased this labelling, i.e. the result indicates TOR phosphorylates TRPML1 at Ser^{572} and Ser^{576}.

DISCUSSION

Through the present study, we have provided evidence that the TRPML1 channel is directly phosphorylated and regulated by the TOR kinase but that AMPK could still be involved indirectly through activity on the TOR pathway (Table 1, Figure 6; [58,59]). Because AMPK also regulates autophagy, it is possible that we detected the genetic interaction between *AMPK* and *MCOLN1*. The general role of TOR in autophagy is well-documented in the literature [60]; however, obtaining mechanistic information on signalling events occurring during autophagy in MLIV is currently a very active area of study [61] and was further elucidated by the present study.

When mutated to phosphomimetic residues (serine to glutamic acid), the C-terminal tail of the channel proved to contain functionally important serine residues (Ser^{572} and Ser^{576}). This finding validates and expands upon previous studies that have strongly suggested links between TOR and the endocytic system, e.g. TOR has been localized to endocytic membranes in yeast, fly and in mammalian cell culture [62–64]. These types of regulatory findings are neither abundant nor well-characterized in the literature for any of the TRPML channels beyond large-scale MS-based phosphorylation analyses of total cell proteins [65,66]. However, Vergarajauregui et al. [51] did attempt to address whether TRPML1 activity is regulated by phosphorylation.

In one study [51], those authors identified two PKA (protein kinase A) consensus motifs in the C-terminal tail of TRPML1, containing Ser^{557} and Ser^{559}. In addition, they found that activation of PKA with forskolin promoted TRPML1 phosphorylation whereas the addition of the PKA inhibitor H-89 abolished TRPML1 phosphorylation and that PKA-mediated phosphorylation regulated TRPML1 channel activity, i.e. forskolin treatment decreased TRPML1 channel activity whereas treatment with H-89 increased TRPML1 channel activity.

Unfortunately, the PKA inhibitor H-89 also inhibits several other kinases (e.g., S6K1, MSK1 [mitogen- and stress-activated protein kinase 1], PKA, ROCKII [rho-associated protein kinase II], PKBα [protein kinase Bα] and MAPKAP-K1b [MAPK (mitogen-activated protein kinase)-activated protein kinase-1b]) [67–69] through its competitive inhibition of the ATP site [70] and forskolin resensitizes cell receptors by activating adenylyl cyclase and increases the intracellular levels of cAMP, thereby activating cAMP-sensitive pathways, such as PKA [71]. Thus, the lack of specificity of the PKA activator and inhibitor (forskolin and H-89) make these results more difficult to interpret. However, it should be noted that the stimulatory effect of H-89 on TRPML1 function was not observed when Ser^{557} and Ser^{559} were mutated to alanine residues, indicating that these two residues may be involved in the negative regulation of TRPML1 [51].

Our results also indicate the negative regulation of TRPML1 due to the phosphorylation of serine residues (however Ser^{572} and Ser^{576} and not Ser^{557} or Ser^{559}), which also decreases functional autophagy, illustrated by the lack of LC3-II turnover in the S572E/S576E mutant (a characteristic of MLIV patients [72], the *MCOLN1*$^{-/-}$ mouse model [33,34] and lysosomal storage diseases in general [73]) and by direct Ca^{2+} imaging using a specific TRPML1 agonist, ML-SA1 [39]. Thus, our results support the typical MLIV pathophysiology and more directly suggest that the phosphorylation of Ser^{572} and Ser^{576} regulate the TRPML1 channel.

In general, LSDs, a group of over 60 genetic conditions [74], are due to lysosomal hydrolase deficiencies that lead to accumulations of their corresponding substrates within lysosomes [25,26], with mucolipidosis types I – III falling into this particular and prevalent category of LSDs. This fact makes the occurrence of MLIV the more interesting because it is due to a loss-of-function of a presumed Ca^{2+} channel, which is a mechanism of autophagy regulation with some support in the literature, i.e. the exocytosis of lysosomal contents is thought to be regulated by the release of intralysosomal Ca^{2+} into the cytosol [75–77]. Thus, our work expands upon our knowledge of TRP channel regulation by protein kinases in general, an area of study that does exist [78–81] but that is lacking for the TRPML channels, and may aid in the development of treatments for inducing autophagy activation, a proposed therapeutic strategy for the treatment of neurodegenerative diseases [82].

AUTHOR CONTRIBUTION

Rob Onyenwoke designed the experiments, collected the data and wrote the paper. Jonathan Sexton collected and analysed the data and reviewed the manuscript. Feng Yan collected and analysed the data; María Díaz collected the data. Lawrence Forsberg collected and analysed the data. Michael Major designed the experiments and reviewed the manuscript. Jay Brenman designed the experiments, wrote the paper and reviewed the manuscript.

ACKNOWLEDGEMENTS

We thank R. Puertollano (NIH, Bethesda, MD) for the pEGFPC2-MCOLN1 construct and D. Kretzschmar (Oregon Health and Science University, Portland, Oregon) and C. Montell (University of California-Santa Barbara, CA) for the *UAS-SNF4* and *trpml*^{2} fly lines respectively. We are also indebted to Professor Robert Tarran (UNC-Chapel Hill) for assistance with the confocal imaging experiments. The authors declare that they have no competing interests.

FUNDING

This work was supported by grants from the state of North Carolina (University Cancer Research Fund); and the National Institute of Health [grant number 1-DP2-OD007149-01 (to M.B.M) and NS080108 (to J.E.B)].

REFERENCES

1 Klionsky, D.J. (2007) Autophagy: from phenomenology to molecular understanding in less than a decade. Nat. Rev. Mol. Cell Biol. **8**, 931–937 CrossRef PubMed

2 Rubinsztein, D.C. (2006) The roles of intracellular protein-degradation pathways in neurodegeneration. Nature **443**, 780–786 CrossRef PubMed
3 Fader, C.M. and Colombo, M.I. (2009) Autophagy and multivesicular bodies: two closely related partners. Cell Death Differ **16**, 70–78 CrossRef PubMed
4 Metcalf, D. and Isaacs, A.M. (2010) The role of ESCRT proteins in fusion events involving lysosomes, endosomes and autophagosomes. Biochem. Soc. Trans. **38**, 1469–1473 CrossRef PubMed
5 Komatsu, M., Waguri, S., Chiba, T., Murata, S., Iwata, J., Tanida, I., Ueno, T., Koike, M., Uchiyama, Y., Kominami, E. and Tanaka, K. (2006) Loss of autophagy in the central nervous system causes neurodegeneration in mice. Nature **441**, 880–884 CrossRef PubMed
6 Williams, A., Jahreiss, L., Sarkar, S., Saiki, S., Menzies, F.M., Ravikumar, B. and Rubinsztein, D.C. (2006) Aggregate-prone proteins are cleared from the cytosol by autophagy: therapeutic implications. Curr. Top. Dev. Biol. **76**, 89–101 CrossRef PubMed
7 Wang, Z., Wilson, W.A., Fujino, M.A. and Roach, P.J. (2001) Antagonistic controls of autophagy and glycogen accumulation by Snf1p, the yeast homolog of AMP-activated protein kinase, and the cyclin-dependent kinase Pho85p. Mol. Cell. Biol. **21**, 5742–5752 CrossRef PubMed
8 Liang, J., Shao, S.H., Xu, Z.X., Hennessy, B., Ding, Z., Larrea, M., Kondo, S., Dumont, D.J., Gutterman, J.U., Walker, C.L. et al. (2007) The energy sensing LKB1-AMPK pathway regulates p27(kip1) phosphorylation mediating the decision to enter autophagy or apoptosis. Nat. Cell Biol. **9**, 218–224 CrossRef PubMed
9 Matsui, Y., Takagi, H., Qu, X., Abdellatif, M., Sakoda, H., Asano, T., Levine, B. and Sadoshima, J. (2007) Distinct roles of autophagy in the heart during ischemia and reperfusion: roles of AMP-activated protein kinase and Beclin 1 in mediating autophagy. Circ. Res. **100**, 914–922 CrossRef PubMed
10 Meley, D., Bauvy, C., Houben-Weerts, J.H., Dubbelhuis, P.F., Helmond, M.T., Codogno, P. and Meijer, A.J. (2006) AMP-activated protein kinase and the regulation of autophagic proteolysis. J. Biol. Chem. **281**, 34870–34879 CrossRef PubMed
11 Samari, H.R. and Seglen, P.O. (1998) Inhibition of hepatocytic autophagy by adenosine, aminoimidazole-4-carboxamide riboside, and N6-mercaptopurine riboside. Evidence for involvement of amp-activated protein kinase. J. Biol. Chem. **273**, 23758–23763
12 Samari, H.R., Moller, M.T., Holden, L., Asmyhr, T. and Seglen, P.O. (2005) Stimulation of hepatocytic AMP-activated protein kinase by okadaic acid and other autophagy-suppressive toxins. Biochem. J. **386**, 237–244 CrossRef PubMed
13 Inoki, K., Zhu, T. and Guan, K.L. (2003) TSC2 mediates cellular energy response to control cell growth and survival. Cell **115**, 577–590 CrossRef PubMed
14 Cheng, S.W., Fryer, L.G., Carling, D. and Shepherd, P.R. (2004) Thr2446 is a novel mammalian target of rapamycin (mTOR) phosphorylation site regulated by nutrient status. J. Biol. Chem. **279**, 15719–15722 CrossRef PubMed
15 Bohensky, J., Leshinsky, S., Srinivas, V. and Shapiro, I.M. (2010) Chondrocyte autophagy is stimulated by HIF-1 dependent AMPK activation and mTOR suppression. Pediatr. Nephrol. **25**, 633–642 CrossRef PubMed
16 Tschape, J.A., Hammerschmied, C., Muhlig-Versen, M., Athenstaedt, K., Daum, G. and Kretzschmar, D. (2002) The neurodegeneration mutant lochrig interferes with cholesterol homeostasis and Appl processing. EMBO J **21**, 6367–6376 CrossRef PubMed
17 Spasic, M.R., Callaerts, P. and Norga, K.K. (2008) Drosophila alicorn is a neuronal maintenance factor protecting against activity-induced retinal degeneration. J. Neurosci. **28**, 6419–6429 CrossRef PubMed
18 Lessing, D. and Bonini, N.M. (2009) Maintaining the brain: insight into human neurodegeneration from *Drosophila melanogaster* mutants. Nat. Rev. Genet. **10**, 359–370 CrossRef PubMed
19 Andersen, R.O., Turnbull, D.W., Johnson, E.A. and Doe, C.Q. (2012) Sgt1 acts via an LKB1/AMPK pathway to establish cortical polarity in larval neuroblasts. Dev. Biol. **363**, 258–265 CrossRef PubMed
20 Swick, L.L., Kazgan, N., Onyenwoke, R.U. and Brenman, J.E. (2013) Isolation of AMP-activated protein kinase (AMPK) alleles required for neuronal maintenance in *Drosophila melanogaster*. Biol. Open **2**, 1321–1323 CrossRef PubMed
21 Bargal, R., Avidan, N., Ben-Asher, E., Olender, Z., Zeigler, M., Frumkin, A., Raas-Rothschild, A., Glusman, G., Lancet, D. and Bach, G. (2000) Identification of the gene causing mucolipidosis type IV. Nat. Genet. **26**, 118–123 CrossRef PubMed
22 Sun, M., Goldin, E., Stahl, S., Falardeau, J.L., Kennedy, J.C., Acierno, Jr, J.S., Bove, C., Kaneski, C.R., Nagle, J., Bromley, M.C. et al. (2000) Mucolipidosis type IV is caused by mutations in a gene encoding a novel transient receptor potential channel. Hum. Mol. Genet. **9**, 2471–2478 CrossRef PubMed
23 Berman, E.R., Livni, N., Shapira, E., Merin, S. and Levij, I.S. (1974) Congenital corneal clouding with abnormal systemic storage bodies: a new variant of mucolipidosis. J. Pediatr. **84**, 519–526 CrossRef PubMed
24 Merin, S., Livni, N., Berman, E.R. and Yatziv, S. (1975) Mucolipidosis IV: ocular, systemic, and ultrastructural findings. Invest. Ophthalmol. **14**, 437–448 PubMed
25 Chen, C.S., Bach, G. and Pagano, R.E. (1998) Abnormal transport along the lysosomal pathway in mucolipidosis, type IV disease. Proc. Natl. Acad. Sci. U.S.A. **95**, 6373–6378 CrossRef PubMed
26 Bargal, R. and Bach, G. (1997) Mucolipidosis type IV: abnormal transport of lipids to lysosomes. J. Inherit. Metab. Dis. **20**, 625–632 CrossRef PubMed
27 Goebel, H.H., Kohlschutter, A. and Lenard, H.G. (1982) Morphologic and chemical biopsy findings in mucolipidosis IV. Clin. Neuropathol. **1**, 73–82 PubMed
28 Folkerth, R.D., Alroy, J., Lomakina, I., Skutelsky, E., Raghavan, S.S. and Kolodny, E.H. (1995) Mucolipidosis IV: morphology and histochemistry of an autopsy case. J. Neuropathol. Exp. Neurol. **54**, 154–164 CrossRef PubMed
29 Bargal, R. and Bach, G. (1988) Phospholipids accumulation in mucolipidosis IV cultured fibroblasts. J. Inherit. Metab. Dis. **11**, 144–150 CrossRef PubMed
30 Goldin, E., Blanchette-Mackie, E.J., Dwyer, N.K., Pentchev, P.G. and Brady, R.O. (1995) Cultured skin fibroblasts derived from patients with mucolipidosis 4 are auto-fluorescent. Pediatr. Res. **37**, 687–692 CrossRef PubMed
31 Bargal, R. and Bach, G. (1989) Phosphatidylcholine storage in mucolipidosis IV. Clin. Chim. Acta **181**, 167–174 CrossRef PubMed
32 Venugopal, B., Browning, M.F., Curcio-Morelli, C., Varro, A., Michaud, N., Nanthakumar, N., Walkley, S.U., Pickel, J. and Slaugenhaupt, S.A. (2007) Neurologic, gastric, and opthalmologic pathologies in a murine model of mucolipidosis type IV. Am. J. Hum. Genet. **81**, 1070–1083 CrossRef PubMed
33 Micsenyi, M.C., Dobrenis, K., Stephney, G., Pickel, J., Vanier, M.T., Slaugenhaupt, S.A. and Walkley, S.U. (2009) Neuropathology of the Mcoln1(− / −) knockout mouse model of mucolipidosis type IV. J. Neuropathol. Exp. Neurol. **68**, 125–135 CrossRef PubMed
34 Curcio-Morelli, C., Charles, F.A., Micsenyi, M.C., Cao, Y., Venugopal, B., Browning, M.F., Dobrenis, K., Cotman, S.L., Walkley, S.U. and Slaugenhaupt, S.A. (2010) Macroautophagy is defective in mucolipin-1-deficient mouse neurons. Neurobiol. Dis. **40**, 370–377 CrossRef PubMed
35 Choi, Y.J., Park, Y.J., Park, J.Y., Jeong, H.O., Kim, D.H., Ha, Y.M., Kim, J.M., Song, Y.M., Heo, H.S., Yu, B.P. et al. (2012) Inhibitory effect of mTOR activator MHY1485 on autophagy: suppression of lysosomal fusion. PLoS One **7**, e43418 CrossRef PubMed
36 Vergarajauregui, S. and Puertollano, R. (2006) Two di-leucine motifs regulate trafficking of mucolipin-1 to lysosomes. Traffic **7**, 337–353 CrossRef PubMed
37 Kazgan, N., Williams, T., Forsberg, L.J. and Brenman, J.E. (2010) Identification of a nuclear export signal in the catalytic subunit of AMP-activated protein kinase. Mol. Biol. Cell **21**, 3433–3442 CrossRef PubMed
38 Dong, X.P., Wang, X., Shen, D., Chen, S., Liu, M., Wang, Y., Mills, E., Cheng, X., Delling, M. and Xu, H. (2009) Activating mutations of the TRPML1 channel revealed by proline-scanning mutagenesis. J. Biol. Chem. **284**, 32040–32052 CrossRef PubMed
39 Shen, D., Wang, X., Li, X., Zhang, X., Yao, Z., Dibble, S., Dong, X.P., Yu, T., Lieberman, A.P., Showalter, H.D. and Xu, H. (2012) Lipid storage disorders block lysosomal trafficking by inhibiting a TRP channel and lysosomal calcium release. Nat. Commun. **3**, 731 CrossRef PubMed
40 Barreto-Chang, O.L. and Dolmetsch, R.E. (2009) Calcium imaging of cortical neurons using Fura-2 AM. J. Vis. Exp. **23**, pii: 1067
41 Kamentsky, L., Jones, T.R., Fraser, A., Bray, M.A., Logan, D.J., Madden, K.L., Ljosa, V., Rueden, C., Eliceiri, K.W. and Carpenter, A.E. (2011) Improved structure, function and compatibility for CellProfiler: modular high-throughput image analysis software. Bioinformatics **27**, 1179–1180 CrossRef PubMed
42 Davies, S.P., Carling, D. and Hardie, D.G. (1989) Tissue distribution of the AMP-activated protein kinase, and lack of activation by cyclic-AMP-dependent protein kinase, studied using a specific and sensitive peptide assay. Eur. J. Biochem. **186**, 123–128 CrossRef PubMed
43 Mahfouz, M.M., Kim, S., Delauney, A.J. and Verma, D.P. (2006) Arabidopsis TARGET OF RAPAMYCIN interacts with RAPTOR, which regulates the activity of S6 kinase in response to osmotic stress signals. Plant Cell **18**, 477–490 CrossRef PubMed
44 Bonini, N.M. and Fortini, M.E. (2003) Human neurodegenerative disease modeling using *Drosophila*. Annu. Rev. Neurosci. **26**, 627–656 CrossRef PubMed
45 Venkatachalam, K., Long, A.A., Elsaesser, R., Nikolaeva, D., Broadie, K. and Montell, C. (2008) Motor deficit in a *Drosophila* model of mucolipidosis type IV due to defective clearance of apoptotic cells. Cell **135**, 838–851 CrossRef PubMed
46 Johnson, E.C., Kazgan, N., Bretz, C.A., Forsberg, L.J., Hector, C.E., Worthen, R.J., Onyenwoke, R. and Brenman, J.E. (2010) Altered metabolism and persistent starvation behaviors caused by reduced AMPK function in *Drosophila*. PLoS One **5**, pii: e12799
47 Onyenwoke, R.U., Forsberg, L.J., Liu, L., Williams, T., Alzate, O. and Brenman, J.E. (2012) AMPK directly inhibits NDPK through a phosphoserine switch to maintain cellular homeostasis. Mol. Biol. Cell **23**, 381–389 CrossRef PubMed
48 Montagne, J., Stewart, M.J., Stocker, H., Hafen, E., Kozma, S.C. and Thomas, G. (1999) *Drosophila* S6 kinase: a regulator of cell size. Science **285**, 2126–2129 CrossRef PubMed
49 Kiselyov, K., Chen, J., Rbaibi, Y., Oberdick, D., Tjon-Kon-Sang, S., Shcheynikov, N., Muallem, S. and Soyombo, A. (2005) TRP-ML1 is a lysosomal monovalent cation channel that undergoes proteolytic cleavage. J. Biol. Chem. **280**, 43218–43223 CrossRef PubMed

50 Soyombo, A.A., Tjon-Kon-Sang, S., Rbaibi, Y., Bashllari, E., Bisceglia, J., Muallem, S. and Kiselyov, K. (2006) TRP-ML1 regulates lysosomal pH and acidic lysosomal lipid hydrolytic activity. J. Biol. Chem. **281**, 7294–7301 CrossRef PubMed

51 Vergarajauregui, S., Oberdick, R., Kiselyov, K. and Puertollano, R. (2008) Mucolipin 1 channel activity is regulated by protein kinase A-mediated phosphorylation. Biochem. J. **410**, 417–425 CrossRef PubMed

52 Lee, M., Hwang, J.T., Lee, H.J., Jung, S.N., Kang, I., Chi, S.G., Kim, S.S. and Ha, J. (2003) AMP-activated protein kinase activity is critical for hypoxia-inducible factor-1 transcriptional activity and its target gene expression under hypoxic conditions in DU145 cells. J. Biol. Chem. **278**, 39653–39661 CrossRef PubMed

53 Kabeya, Y., Mizushima, N., Ueno, T., Yamamoto, A., Kirisako, T., Noda, T., Kominami, E., Ohsumi, Y. and Yoshimori, T. (2000) LC3, a mammalian homologue of yeast Apg8p, is localized in autophagosome membranes after processing. EMBO J **19**, 5720–5728 CrossRef PubMed

54 Tanida, I., Minematsu-Ikeguchi, N., Ueno, T. and Kominami, E. (2005) Lysosomal turnover, but not a cellular level, of endogenous LC3 is a marker for autophagy. Autophagy **1**, 84–91 CrossRef PubMed

55 Williams, T., Forsberg, L.J., Viollet, B. and Brenman, J.E. (2009) Basal autophagy induction without AMP-activated protein kinase under low glucose conditions. Autophagy **5**, 1155–1165 CrossRef PubMed

56 Mizushima, N. and Yoshimori, T. (2007) How to interpret LC3 immunoblotting. Autophagy **3**, 542–545 CrossRef PubMed

57 Tanida, I., Ueno, T. and Kominami, E. (2008) LC3 and Autophagy. Methods Mol. Biol. **445**, 77–88 CrossRef PubMed

58 Wong, C.O., Li, R., Montell, C. and Venkatachalam, K. (2012) *Drosophila* TRPML is required for TORC1 activation. Curr. Biol. **22**, 1616–1621 CrossRef PubMed

59 Venkatachalam, K., Wong, C.O. and Montell, C. (2013) Feast or famine: role of TRPML in preventing cellular amino acid starvation. Autophagy **9**, 98–100 CrossRef PubMed

60 Alers, S., Loffler, A.S., Wesselborg, S. and Stork, B. (2012) Role of AMPK-mTOR-Ulk1/2 in the regulation of autophagy: cross talk, shortcuts, and feedbacks. Mol. Cell. Biol. **32**, 2–11 CrossRef PubMed

61 Zoncu, R., Efeyan, A. and Sabatini, D.M. (2011) mTOR: from growth signal integration to cancer, diabetes and ageing. Nat. Rev. Mol. Cell Biol. **12**, 21–35 CrossRef PubMed

62 Sancak, Y., Peterson, T.R., Shaul, Y.D., Lindquist, R.A., Thoreen, C.C., Bar-Peled, L. and Sabatini, D.M. (2008) The Rag GTPases bind raptor and mediate amino acid signaling to mTORC1. Science **320**, 1496–1501 CrossRef PubMed

63 Kunz, J., Schneider, U., Howald, I., Schmidt, A. and Hall, M.N. (2000) HEAT repeats mediate plasma membrane localization of Tor2p in yeast. J. Biol. Chem. **275**, 37011–37020 CrossRef PubMed

64 Wedaman, K.P., Reinke, A., Anderson, S., Yates, III, J., McCaffery, J.M. and Powers, T. (2003) Tor kinases are in distinct membrane-associated protein complexes in *Saccharomyces cerevisiae*. Mol. Biol. Cell **14**, 1204–1220 CrossRef PubMed

65 Trost, M., English, L., Lemieux, S., Courcelles, M., Desjardins, M. and Thibault, P. (2009) The phagosomal proteome in interferon-gamma-activated macrophages. Immunity **30**, 143–154 CrossRef PubMed

66 Ballif, B.A., Villen, J., Beausoleil, S.A., Schwartz, D. and Gygi, S.P. (2004) Phosphoproteomic analysis of the developing mouse brain. Mol. Cell. Proteomics **3**, 1093–1101 CrossRef PubMed

67 Marunaka, Y. and Niisato, N. (2003) H89, an inhibitor of protein kinase A (PKA), stimulates Na + transport by translocating an epithelial Na + channel (ENaC) in fetal rat alveolar type II epithelium. Biochem. Pharmacol. **66**, 1083–1089 CrossRef PubMed

68 Lochner, A. and Moolman, J.A. (2006) The many faces of H89: a review. Cardiovasc. Drug Rev. **24**, 261–274 CrossRef PubMed

69 Cho, I.J., Woo, N.R., Shin, I.C. and Kim, S.G. (2009) H89, an inhibitor of PKA and MSK, inhibits cyclic-AMP response element binding protein-mediated MAPK phosphatase-1 induction by lipopolysaccharide. Inflamm. Res. **58**, 863–872 CrossRef PubMed

70 Murray, A.J. (2008) Pharmacological PKA inhibition: all may not be what it seems. Sci. Signal. **1**, re4 CrossRef PubMed

71 Alasbahi, R.H. and Melzig, M.F. (2012) Forskolin and derivatives as tools for studying the role of cAMP. Die Pharmazie **67**, 5–13 PubMed

72 Vergarajauregui, S., Connelly, P.S., Daniels, M.P. and Puertollano, R. (2008) Autophagic dysfunction in mucolipidosis type IV patients. Hum. Mol. Genet. **17**, 2723–2737 CrossRef PubMed

73 Yue, Z., Friedman, L., Komatsu, M. and Tanaka, K. (2009) The cellular pathways of neuronal autophagy and their implication in neurodegenerative diseases. Biochim. Biophys. Acta **1793**, 1496–1507 CrossRef PubMed

74 Raben, N., Shea, L., Hill, V. and Plotz, P. (2009) Monitoring autophagy in lysosomal storage disorders. Methods Enzymol **453**, 417–449 CrossRef PubMed

75 Luzio, J.P., Bright, N.A. and Pryor, P.R. (2007) The role of calcium and other ions in sorting and delivery in the late endocytic pathway. Biochem. Soc. Trans. **35**, 1088–1091 CrossRef PubMed

76 Pryor, P.R., Mullock, B.M., Bright, N.A., Gray, S.R. and Luzio, J.P. (2000) The role of intraorganellar Ca(2 +) in late endosome-lysosome heterotypic fusion and in the reformation of lysosomes from hybrid organelles. J. Cell Biol. **149**, 1053–1062 CrossRef PubMed

77 Reddy, A., Caler, E.V. and Andrews, N.W. (2001) Plasma membrane repair is mediated by Ca(2 +)-regulated exocytosis of lysosomes. Cell **106**, 157–169 CrossRef PubMed

78 Nilius, B., Prenen, J., Tang, J., Wang, C., Owsianik, G., Janssens, A., Voets, T. and Zhu, M.X. (2005) Regulation of the Ca^{2+} sensitivity of the nonselective cation channel TRPM4. J. Biol. Chem. **280**, 6423–6433 CrossRef PubMed

79 Jiang, X., Newell, E.W. and Schlichter, L.C. (2003) Regulation of a TRPM7-like current in rat brain microglia. J. Biol. Chem. **278**, 42867–42876 CrossRef PubMed

80 Vazquez, G., Wedel, B.J., Kawasaki, B.T., Bird, G.S. and Putney, Jr, J.W. (2004) Obligatory role of Src kinase in the signaling mechanism for TRPC3 cation channels. J. Biol. Chem. **279**, 40521–40528 CrossRef PubMed

81 Venkatachalam, K., Zheng, F. and Gill, D.L. (2003) Regulation of canonical transient receptor potential (TRPC) channel function by diacylglycerol and protein kinase C. J. Biol. Chem. **278**, 29031–29040 CrossRef PubMed

82 Garcia-Arencibia, M., Hochfeld, W.E., Toh, P.P. and Rubinsztein, D.C. (2010) Autophagy, a guardian against neurodegeneration. Semin. Cell Dev. Biol. **21**, 691–698 CrossRef PubMed

Received 13 March 2015/17 July 2015; accepted 20 July 2015
Accepted Manuscript online 20 July 2015, doi:10.1042/BJ20150219